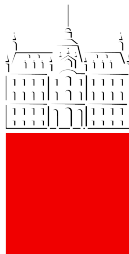


University of Ljubljana  
Faculty of Mathematics and Physics



Master program in Physics  
Seminar 2

# Quantum simulator using Rydberg atoms in optical tweezers

Author: Katja Gosar  
Advisor: dr. Peter Jeglič

Ljubljana, April 14th 2021

## Abstract

Optical tweezers are tightly focused optical dipole traps with controllable trapping position. First, we present an experimental protocol for creating a defect-free array of single rubidium atoms held in optical tweezers. Then, we present the properties and interactions of Rydberg states. We describe how Rydberg interactions in an array of cold atoms make a controllable and flexible system that is used as a quantum simulator. Finally, we discuss the observed phase diagram and phase transitions.

# Contents

<b>1</b>	<b>Introduction</b>	<b>2</b>
<b>2</b>	<b>Atoms in optical tweezers</b>	<b>3</b>
2.1	Dipole traps . . . . .	3
2.2	Optical tweezers . . . . .	3
2.3	Preparation of defect-free atom arrays . . . . .	5
<b>3</b>	<b>Rydberg atoms</b>	<b>6</b>
3.1	Basic properties of Rydberg atoms . . . . .	6
3.2	Rydberg state excitation and Rabi oscillations . . . . .	6
3.3	Dipole-dipole interactions . . . . .	6
3.4	Rydberg blockade . . . . .	7
<b>4</b>	<b>Quantum simulator</b>	<b>8</b>
4.1	Experiment . . . . .	8
4.2	Hamiltonian . . . . .	9
4.3	Phase diagram . . . . .	10
4.4	Phase transitions . . . . .	11
<b>5</b>	<b>Conclusions</b>	<b>11</b>

## 1 Introduction

Quantum physics introduces concepts like superposition and entanglement that quantum technologies utilize to perform tasks that are classically impossible or hard to do. Quantum technologies include quantum computing, communication, simulation, sensing and metrology. For most kinds of quantum technologies we need quantum systems that consist of several well-controlled elements that interact with each other [1]. The purpose of quantum simulation is to use a synthetic quantum system to study a model Hamiltonian of a real-world physical problem, that is hard to solve with classical computing [2]. One of the platforms for quantum simulation are neutral atoms at very low temperatures. The atoms are controlled via optical and electromagnetic methods, particularly through the interaction of Rydberg states. The advantage of cold neutral atoms is that they are inherently identical, and it is easy to scale up the systems to large numbers of atoms [2].

In this seminar, we focus on quantum simulations based on atoms held in optical tweezers. In the first section, we present dipole-trapping of atoms and how optical tweezers can be used to create arrays of atoms. Next, we present Rydberg atoms as a state with strong and controllable interactions. Lastly, we present the experiments from Ref. [3], where they used an array of neutral atoms with Rydberg excitations as a quantum simulator to probe the many-body dynamics of the engineered Hamiltonian.

## 2 Atoms in optical tweezers

### 2.1 Dipole traps

Atoms can be trapped using optical dipole traps. Those are focused beams of far off-resonant light that create an attracting potential for the atoms. Because the light is off-resonant, optical excitations do not play a role in this case. The light intensity and detuning is chosen such that the radiation force due to photon scattering is negligible compared to the dipole force.

Consider an atom in a laser beam with the frequency  $\omega$ , polarization  $\hat{\mathbf{e}}$  and amplitude  $E$ . The electric field  $\mathbf{E}(\mathbf{r}, t) = \hat{\mathbf{e}}E \exp(-i\omega t) + c. c.$  induces an atomic dipole moment  $\mathbf{p}(\mathbf{r}, t) = \hat{\mathbf{e}}p \exp(-i\omega t) + c. c.$ . The amplitude of the dipole moment  $p = \alpha E$  is proportional to the electric field amplitude  $E$ , where  $\alpha$  is the complex polarizability that is a function of  $\omega$  [4]. We can express the interaction potential of the induced dipole moment as

$$U_{\text{dip}} = -\frac{1}{2} \langle \mathbf{p} \mathbf{E} \rangle = -\frac{1}{2\epsilon_0 c} \text{Re}(\alpha) I, \quad (1)$$

where we took the time average over the rapid oscillations of the field and introduced the field intensity as  $I = 2\epsilon_0 c |E|^2$ . The dipole force due to this potential is [4]

$$\mathbf{F}_{\text{dip}}(\mathbf{r}) = -\nabla U_{\text{dip}}(\mathbf{r}) = \frac{1}{2\epsilon_0 c} \text{Re}(\alpha) \nabla I(\mathbf{r}). \quad (2)$$

The atomic polarizability  $\alpha$  can be calculated using Lorentz's model of a classical oscillator as

$$\alpha = 6\pi\epsilon_0 c^3 \frac{\Gamma/\omega_0^2}{\omega_0^2 - \omega^2 - i(\omega^3/\omega_0^2)\Gamma}, \quad (3)$$

where we introduce the resonance frequency  $\omega_0$  and the damping parameter  $\Gamma$  [4]. This model is in agreement with the quantum description, if the detuning is large enough that the scattering rate is low and there is no saturation effects [4]. In most cases, the driving frequency is tuned relatively close to resonance, such that the detuning  $\Delta = \omega - \omega_0$  is small compared to the resonance frequency  $\omega_0$ , allowing us to use the rotating-wave approximation. In this case, the expression for the dipole potential simplifies to [4]

$$U_{\text{dip}}(\mathbf{r}) = \frac{3\pi c^2}{2\omega_0^3} \frac{\Gamma}{\Delta} I(\mathbf{r}). \quad (4)$$

We can see that the sign of detuning significantly impacts the effect of the light on the atoms. If the frequency is below the atomic resonance ( $\Delta < 0$ ), we say that it is red detuned, and the interaction attracts atoms to points with higher light intensity. However, if the frequency is above resonance ( $\Delta > 0$ ), we say that it is blue detuned and the interaction is repulsive, pushing atoms away from the light field [4].

### 2.2 Optical tweezers

Optical tweezers are tightly focused dipole traps. The position and the intensity is controlled for each trap individually. An array of optical tweezers can be created from a laser beam with an acousto-optic deflector (AOD) and a set of lenses. An example of such a setup is shown in Figure 1. We can see that a laser beam is separated into multiple deflected beams with an AOD. The beams then go through

two lenses in a 1:1 telescope configuration. Then the beams are focused inside the vacuum cell with a microscope objective with a high numerical aperture (NA). The high NA is necessary to create very tightly focused traps. If the trap is small enough, the collisional blockade effect ensures that there can be no more than one single atom in each trap [5, 6]. This is a consequence of a high probability of two-body decay relatively to the loading rate [5]. Two body-decay refers to an atom leaving the trap due to a collision with another atom inside the trap.

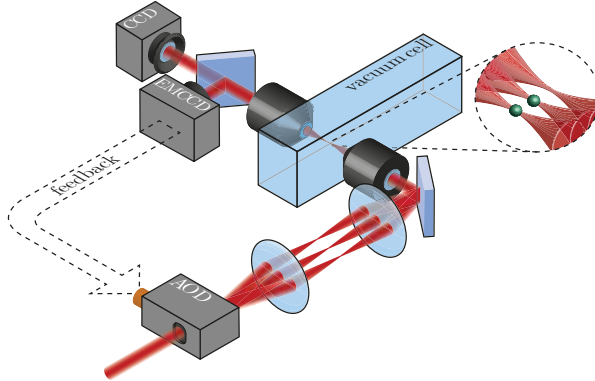


Figure 1: An experimental setup for the preparation of a defect-free atom array. An array of optical tweezers in the vacuum chamber is created with a combination of an AOD, a 1:1 telescope and a high-NA microscope objective. An identical microscope objective on the other side of the vacuum cell is used to image the focal plane of the tweezers. The CCD camera is used to image the tweezers' positions and the EMCCD for the fluorescence imaging. The positions of the atoms are fed back into the AOD in order to re-arrange the trap positions to form a defect-free array. Adapted from Ref. [7].

An AOD is a device that utilizes the acousto-optic effect in a crystal to deflect light. The angle of diffraction is determined by the frequency of the acoustic wave, and the intensity of the diffracted beam depends on the amplitude of the acoustic wave. Figure 2 schematically shows acousto-optic deflection. A piezoelectric transducer transforms the control electrical signal into acoustic waves in the crystal, and the beam of light that goes through the crystal is deflected due to Bragg scattering on the acoustic wave [8].

To create optical tweezers, the AOD is simultaneously driven with multiple frequencies (i. e. multitone driving). Each frequency creates a diffracted beam at its corresponding angle. The tweezer positions can be smoothly moved by sweeping the driving frequency. To turn off or change the intensity of a particular tweezer the amplitude of that frequency component of the driving signal is adjusted [7].

### 2.3 Preparation of defect-free atom arrays

This section describes the preparation of arrays of atoms held in optical tweezers as it is described in Refs. [3] and [7]. The experimental setup is schematically shown in Figure 1 and the procedure in Figure 3.

First,  $^{87}\text{Rb}$  atoms in a vacuum cell are laser-cooled in an magneto-optical trap (MOT). An array of optical tweezers is also turned on during this time. Then, the

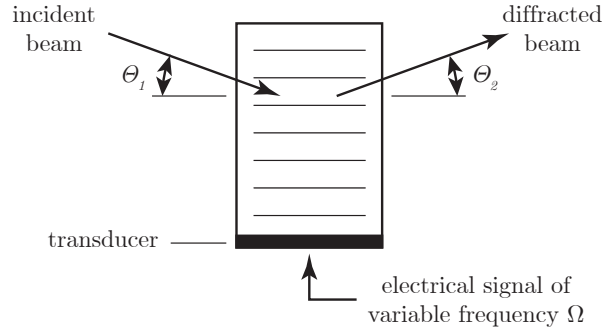


Figure 2: An acousto-optic deflector. The diffraction angle depends on the frequency of the acoustic wave in the crystal. Adapted from Ref. [8].

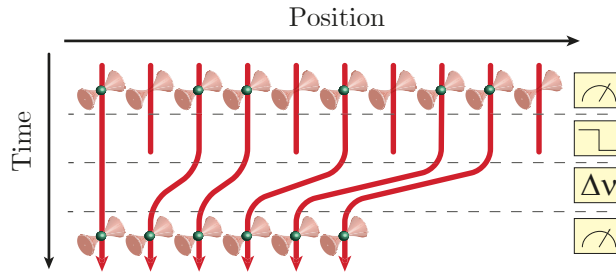


Figure 3: The procedure for creating a defect-free array of atoms. First, the atoms are captured from an MOT with optical tweezers, and the atom positions are imaged. Then, the empty traps are turned off. In the third step, the frequencies corresponding to the filled traps are swept to rearrange the traps into a regular array of filled traps. Adapted from Ref. [7].

MOT is turned off instantaneously and the atomic cloud is left to disperse before fluorescence imaging is used to see which traps are filled with an atom and which are not. The loading of atoms from an MOT into a trap is probabilistic with an efficiency of about 0.6 in this experimental setup [7]. The efficiency depends on the trap intensities and sizes. After the imaging, the empty traps are turned off, and the rest are moved to form a defect-free array of atoms or any other selected pattern. 808-nm light is used for the tweezers, and they have a beam waist of approximately  $0.9 \mu\text{m}$  and the trap depth is approximately  $0.9 \text{ mK}$  [3]. The spacing between the traps can range from a few micrometers to tens of micrometers [3].

Similarly, it is possible to create an arbitrary pattern of atoms in optical tweezers in 2D [9], and even in 3D [10]. The flexibility of the tweezer positions is the main advantage of this method over optical lattices that can similarly be used to create arrays of dipole traps. In that case, the traps are the nodes of an interference pattern of two laser beams [1].

## 3 Rydberg atoms

### 3.1 Basic properties of Rydberg atoms

Rydberg atoms are atoms in states with a high principal quantum number  $n$ , this means, that the valence electron is highly excited [2, 11]. These states have exaggerated properties compared to atoms in the ground state. In particular, they have large dipole moments and strong interactions, making them suitable for many experiments.

Rydberg atoms are very big and have large polarizabilities, leading to large collisional cross sections and long interaction times. The binding energy is very small and the radiative lifetime is very long. This can be understood in the classical electrodynamics picture, where an electron further from the nucleus experiences smaller accelerations and therefore a lower radiation rate [2]. Additionally, Rydberg atoms have big dipole matrix elements that are very sensitive to electric fields [12].

### 3.2 Rydberg state excitation and Rabi oscillations

Consider a two-level system with a ground state  $|g\rangle$  and an excited Rydberg state  $|r\rangle$ , with the energy difference  $\hbar\omega_0$ . A beam of light at frequency  $\omega = \omega_0 + \Delta$ , where  $\Delta$  is the detuning, drives transitions between the two levels in a process called Rabi oscillations. The state of the system oscillates between the two states with the Rabi frequency  $\Omega$  [13]. The Rabi frequency is a function of the intensity of the beam. The detuning  $\Delta$  affects the amplitude of the oscillations. Assume we start with an atom in the ground state  $|g\rangle$ . On resonance ( $\Delta = 0$ ), the probability of finding the atom in the excited state  $|r\rangle$  periodically reaches 1. Off-resonance, the transition to  $|r\rangle$  is never complete, since the amplitude of Rabi oscillations falls with  $|\Delta|$ .

In the experiment described in Ref. [3],  $^{87}\text{Rb}$  atoms are used for quantum simulation. Each of the atoms is effectively a two-level system, with a ground state  $|g\rangle$  and an excited Rydberg state  $|r\rangle$ , but the transition between the states is realized with a two photon process. It uses an intermediate state  $|e\rangle$  as it is schematically shown in Figure 4a. A blue 420-nm laser is used for the  $|g\rangle \rightarrow |e\rangle$  transition, with a detuning  $\delta$  and a Rabi frequency  $\Omega_B$ . For the  $|e\rangle \rightarrow |r\rangle$  transition, an infrared 1013-nm laser is used with a detuning  $\Delta$  and a Rabi frequency  $\Omega_R$ . Because the detuning  $\delta$  is much larger than  $\Omega_B$  and  $\Omega_R$ , the dynamics can be simplified to a two-level transition  $|g\rangle \rightarrow |r\rangle$  with an effective Rabi frequency  $\Omega = \Omega_R\Omega_B/(2\delta)$  [3].

### 3.3 Dipole-dipole interactions

To understand dipole-dipole interactions between Rydberg atoms, we can describe a Rydberg atom as an electric dipole  $\mathbf{p} = -e\mathbf{d}$ , where  $\mathbf{d}$  is the relative displacement of the excited electron from the core. The dipole-dipole interaction between two such atoms is

$$V_{dd} = \frac{e^2}{4\pi\epsilon_0} \frac{\mathbf{d}_1 \cdot \mathbf{d}_2 - 3(\mathbf{d}_1 \cdot \mathbf{e}_R)(\mathbf{d}_2 \cdot \mathbf{e}_R)}{R^3}, \quad (5)$$

where  $\mathbf{e}_R$  is the unit vector along the relative coordinate  $\mathbf{R}$  between the two atoms, and  $R = |\mathbf{R}|$  is the interatomic distance [2, 12].

Consider a case of two atoms with a single transition channel  $|r_1\rangle + |r_2\rangle \rightarrow |r'_1\rangle + |r'_2\rangle$  between (Rydberg) states. It can be shown that the eigenvalues of the

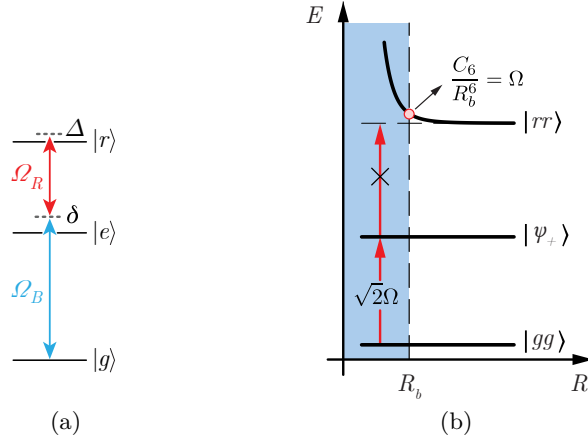


Figure 4: (a) Two photon transition between the ground state and the Rydberg state. Adapted from Ref. [3]. (b) Rydberg blockade results from the energy shift of the doubly-excited state due to the dipole-dipole interaction between Rydberg atoms. If the atoms are closer than  $R_b$ , the excitation of a second atom is off-resonance and therefore greatly suppressed. Adapted from Ref. [2].

Hamiltonian of this system are

$$E_{\pm} = \frac{\delta_F}{2} \pm \frac{1}{2} \sqrt{\delta_F^2 + 4V^2}, \quad (6)$$

where  $\delta_F = (E_{r'_1} + E_{r'_2}) - (E_{r_1} + E_{r_2})$  is the difference between the energies of the initial and final states.  $\delta_F$  is also known as the Förster defect [2].  $V = C_3/R^3$  is the interaction strength for the transition, where  $C_3$  is the anisotropic interaction coefficient, which is a function of the orientation of the two dipoles [2]. We define the interaction induced energy shift as  $\Delta E_{\pm} = E_{\pm}(R) - E_{\pm}(R \rightarrow \infty)$ . We are interested in the case, where  $|r_1\rangle$  and  $|r_2\rangle$  are ground states and  $|r'_1\rangle$  and  $|r'_2\rangle$  are Rydberg states. This means that the energy difference is large,  $\delta_F \gg V(R)$ . It can be shown that, in this limit, the energy shift is  $\Delta E_{-} \approx -C_6/R^6$  for  $|r_1 r_2\rangle$ , and  $\Delta E_{+} \approx C_6/R^6$  for  $|r'_1 r'_2\rangle$ , where  $C_6 = C_3^2/\delta_F$ . In this regime, the interaction is called Van der Waals interaction, because it is proportional to  $R^{-6}$  [2].

### 3.4 Rydberg blockade

Because of the strong dipole-dipole interaction between Rydberg atoms, the excitation to Rydberg states exhibits the behavior that only one atom within a certain volume can be excited. This is called a Rydberg blockade. It occurs because the excited atom shifts the energy of the surrounding atoms, moving the excitation frequency further from resonance [2].

Consider the two atom case illustrated in Figure 4b. The resonant light can excite the atoms into a single-atom excited state  $|\psi_{+}\rangle$ . The energy of the doubly-excited state is shifted due to the dipole-dipole Van der Waals interaction that we described in section 3.3. The interaction is a function of the interatomic distance  $R$ . If  $R$  is smaller than the Rydberg radius  $R_b$ , the light is too far from the shifted resonance, and it can not excite the second atom. The Rydberg radius is defined as the radius where the interaction is equal to the Rabi frequency,  $\Delta E(R_b) = \Omega$  [2, 3]. In the experiment in Ref. [3] the Rydberg radius was 9  $\mu\text{m}$ .

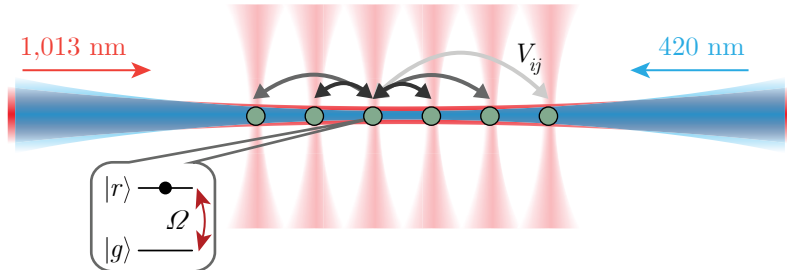


Figure 5: Atoms in optical tweezers and the two beams that induce Rabi oscillations. Adapted from Ref. [3].

Consider  $N$  atoms in a volume with the radius  $R_b$ . A state where all of the atoms within the volume share a single excitation is

$$|W\rangle = \frac{1}{\sqrt{N}} \sum_{i=1}^N |g_1 g_2 \dots r_i \dots g_N\rangle, \quad (7)$$

a superposition of states where one of the atoms is in the excited state. The Rabi frequency between the ground state  $|G\rangle = |g_1 g_2 \dots g_N\rangle$  and  $|W\rangle$  is  $\Omega_N = \sqrt{N}\Omega$ , where  $\Omega$  is the Rabi frequency for a single atom [2, 12]. This can be intuitively understood considering that the probability of excitation increases because any of the  $N$  atoms can be excited.

## 4 Quantum simulator

In the previous sections, we described how one can prepare a defect-free array of atoms in optical tweezers, how these atoms can be excited into Rydberg states and the interaction between them. This is a system that makes an ideal platform for studying quantum many-body dynamics because of its controllability and flexibility. By observing the response of the physical system, we can learn about the properties of the engineered Hamiltonian.

We will focus on Ref. [3], where many-body dynamics was probed on a 51-atom simulator. They used rubidium atoms to create a one dimensional array of 51 atoms. By changing the spacing between the atoms, the detuning of the driving lasers, and the Rabi frequency, different properties of the studied system could be observed.

### 4.1 Experiment

In section 2.3 we described the experimental setup and procedure for creating defect-free atom arrays. Here, we describe the subsequent steps in the quantum simulation experiment.

Figure 5 shows atoms trapped in optical tweezers and the two laser beams necessary for Rydberg state excitation described in section 3.2. Figure 6 shows the four steps of the experiment. First, the atoms are cooled in the MOT and loaded into optical tweezers. Then, the atoms are arranged into regular arrays and imaged to ensure that the traps are still occupied. Afterwards the system is left to evolve for a certain time under the influence of the driving laser beams and without optical

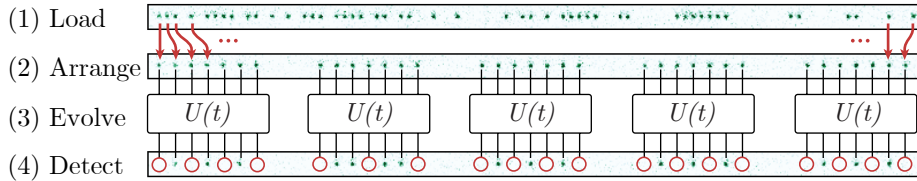


Figure 6: Experimental procedure: the atoms are loaded from an MOT into optical tweezers, the tweezers are rearranged, then the system is left to evolve under the influence of the driving beams, and lastly, the final state is detected. In this case, five independent systems of 7 atoms were studied. Adapted from Ref. [3].

tweezers. Lastly, the tweezers are turned back on, recapturing only the atoms that are still in the ground state. The final occupations are detected with fluorescence imaging.

The time of the free evolution of the system is limited by the thermal motion of the atoms. When the tweezers are turned off, the atoms move freely and will move out of the reach of the tweezers if the evolution time is too long. Only atoms in the ground state are recaptured, because the tweezer's potential is repulsive (anti-trapping) for the Rydberg state.

## 4.2 Hamiltonian

The dynamics of the system is described by the Hamiltonian

$$\frac{H}{\hbar} = \sum_i \frac{1}{2} \Omega_i \sigma_x^i - \sum_i \Delta_i n_i + \sum_{i < j} V_{ij} n_i n_j. \quad (8)$$

The first term describes the coupling between the ground state and the Rydberg state through Rabi oscillations with the frequency  $\Omega_i$ , where  $\sigma_x^i = |g_i\rangle\langle r_i| + |r_i\rangle\langle g_i|$ , where  $i$  indicates the position in the array. The second term comes from the energy of the excited state in the rotating-wave approximation. It is governed by the detuning  $\Delta_i$  from the transition.  $n_i = |r_i\rangle\langle r_i|$  is the operator of the number of atoms in the Rydberg state at position  $i$ . The last term describes the interaction between atoms at different positions. The interaction strength  $V_{ij}$  is controlled through the distance between atoms. In the experiment, the coupling was homogeneous ( $\Omega_i = \Omega$ ,  $\Delta_i = \Delta$ ). In this case, the Hamiltonian is

$$\frac{H}{\hbar} = \Omega \sum_i \frac{1}{2} \sigma_x^i - \Delta \sum_i n_i + \sum_{i < j} V_{ij} n_i n_j \quad (9)$$

and resembles the Ising model for spin-1/2 particles [3].

## 4.3 Phase diagram

The ground state of the Hamiltonian in equation (9) depends on the parameters  $\Omega$ ,  $\Delta$  and  $V_{i,j}$ . If  $\Delta/\Omega$  is negative, the ground state is  $|G\rangle$ , i. e. all atoms in  $|g\rangle$ . If we increase  $\Delta/\Omega$ , the number of atoms in the Rydberg state  $|r\rangle$  will increase. These atoms are regularly distributed across the array, forming a 'Rydberg crystal' [3]. Depending on the interaction range, these crystals exhibit different translational symmetries.

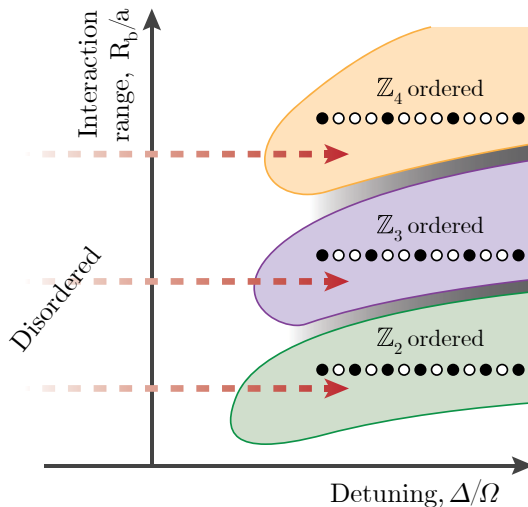


Figure 7: Phase diagram of a one-dimensional array. For lower  $\Delta/\Omega$  the ground state consist of all atoms in  $|g\rangle$ . For higher  $\Delta/\Omega$ , we get crystal phases with different translational symmetries depending on the interaction range. Black circles represent Rydberg states and white circles represent atoms in the ground state. Adapted from Ref. [3].

For example, consider the case when  $\Omega$  is much smaller that the interaction between neighboring atoms  $V_{i,i+1}$ , but much larger then between next-nearest neighbors  $V_{i,i+2}$ . This means that we have Rydberg blockade for neighboring sites, but the next-nearest neighbor interaction is negligible. This results in a ground state where every other atom is in the Rydberg state. This crystal has the  $\mathbb{Z}_2$  translational symmetry. Similarly, if  $V_{i,i+1}, V_{i,i+2} \gg \Omega \gg V_{i,i+3}$ , the ground state has the  $\mathbb{Z}_3$ -symmetry, and every third atom is in the Rydberg state, and so on for higher symmetries. The phase diagram is shown in Figure 7.

#### 4.4 Phase transitions

As it is suggested with red arrows in Figure 7, one can observe phase transitions by slowly changing the detuning across resonance. In Ref. [3], the phase transition to the state with  $\mathbb{Z}_2$  translational symmetry was thoroughly studied.

First, the atoms were prepared with negative detuning with all atoms in the ground state, shown in the first image in Figure 8. Then, the detuning was swept over the resonance and the resulting states were measured [3]. Examples of these are the other three images in Figure 8. We can see that the array consists of sections where atoms alternate between the ground state and the Rydberg state, as they do in the expected ground state. Those sections are separated by domain walls of two neighboring atoms in the same state. In Figure 8, the domain walls are emphasized with blue ellipses.

The mean number of domain walls and its variance was measured as a function of the detuning  $\Delta$ . The results are shown in Figure 9. The system exhibits an Ising-type second-order quantum phase transition. The peak in the variance reflects that, close to the transition point, domains of varying lengths are observed [3].

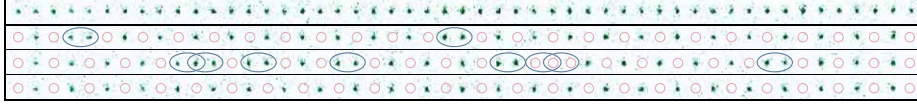


Figure 8: Images of an array of 51 atoms. On the top, an image for negative detuning is shown. Below, there are three instances of the system after the sweep to positive detuning. The domain walls are indicated by blue ellipses. Adapted from [3].

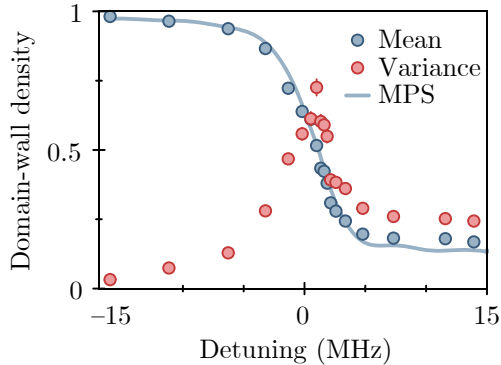


Figure 9: Number of domain walls and its variance as a function of the detuning, clearly showing a phase transition. The blue curve is the theoretically calculated dependence of the mean domain wall density and the dots show the measured values. Adapted from [3].

## 5 Conclusions

Optical tweezers provide a mechanism for the control of individual cold atom positions. The positions are not constrained to any geometry and the atoms can be independently moved with the tweezer. Utilizing the dipole-dipole interaction of Rydberg atoms, we can control the interactions between atoms in neighboring optical traps. This creates a quantum system that can be used as a quantum simulator. Rydberg atom systems naturally map to spin systems [14], like the Ising model in the described example. In addition to observing the phase diagram and phase transitions, the dynamics of the system after a sudden change of the detuning over the phase transition was also studied in Ref. [3]. The research is not limited to the one-dimensional case that we presented, but can extend to two or all three dimensions [14]. In similar setups other phenomena like many-body coherence and entanglement can be studied [3]. There is also the possibility to study topological states, nonequilibrium dynamics of systems and to test the Kibble-Zurek mechanism [3]. Quantum simulation can even be used to solve combinatorial optimization problems, for example the traveling salesman's problem [14]. Finally, Rydberg atoms are also a promising platform for quantum computing, since the lattice sites can be individually addressed and the Rydberg blockade provides a mechanism for quantum logical gates [14].

## References

- [1] A. Browaeys, *Alkaline Atoms Held with Optical Tweezers*, Physics **11**, 135 (2018).
- [2] X. Wu, X. Liang, Y. Tian, F. Yang, C. Chen, Y.-C. Liu, M. K. Tey and L. You, *A concise review of Rydberg atom based quantum computation and quantum simulation*, Chinese Physics B **30**, 020305 (2021).
- [3] H. Bernien, S. Schwartz, A. Keesling, H. Levine, A. Omran, H. Pichler, S. Choi, A. S. Zibrov, M. Endres, M. Greiner *et al.*, *Probing many-body dynamics on a 51-atom quantum simulator*, Nature **551**, 579 (2017).
- [4] R. Grimm, M. Weidemüller and Y. B. Ovchinnikov, *Optical dipole traps for neutral atoms*, Advances in atomic, molecular, and optical physics **42**, 95 (2000).
- [5] N. Schlosser, G. Reymond and P. Grangier, *Collisional blockade in microscopic optical dipole traps*, Physical review letters **89**, 023005 (2002).
- [6] M. Weber, J. Volz, K. Saucke, C. Kurtsiefer and H. Weinfurter, *Analysis of a single-atom dipole trap*, Physical Review A **73**, 043406 (2006).
- [7] M. Endres, H. Bernien, A. Keesling, H. Levine, E. R. Anschuetz, A. Krajenbrink, C. Senko, V. Vuletic, M. Greiner and M. D. Lukin, *Atom-by-atom assembly of defect-free one-dimensional cold atom arrays*, Science **354**, 1024 (2016).
- [8] R. W. Boyd, *Nonlinear optics* (Academic press, 2020).
- [9] D. Barredo, S. De Léséleuc, V. Lienhard, T. Lahaye and A. Browaeys, *An atom-by-atom assembler of defect-free arbitrary two-dimensional atomic arrays*, Science **354**, 1021 (2016).
- [10] D. Barredo, V. Lienhard, S. De Leseleuc, T. Lahaye and A. Browaeys, *Synthetic three-dimensional atomic structures assembled atom by atom*, Nature **561**, 79 (2018).
- [11] T. F. Gallagher, *Rydberg atoms*, 3 (Cambridge University Press, 2005).
- [12] D. Comparat and P. Pillet, *Dipole blockade in a cold Rydberg atomic sample*, Journal of the Optical Society of America B **27**, A208 (2010).
- [13] D. J. Griffiths and D. F. Schroeter, *Introduction to quantum mechanics* (Cambridge University Press, 2018).
- [14] A. Browaeys and T. Lahaye, *Many-body physics with individually controlled Rydberg atoms*, Nature Physics **16**, 132 (2020).